

width=.75

Electronic Supplementary Material

Prediction of Improved Thermoelectric Performance by Ordering in Double Half-Heusler Materials

Shuping Guo,^{a,b,d} Zihang Liu,^c Zhenzhen Feng,^e Tiantian Jia,^{a,d} Shashwat Anand,^b G. Jeffrey
Snyder^{*b} and Yongsheng Zhang^{*a,d}

^aKey Laboratory of Materials Physics, Institute of Solid State Physics, HFIPS, Chinese Academy of Sciences, Hefei 230031, China.

^bDepartment of Materials Science and Engineering, Northwestern University, Evanston, IL 60208, USA

^cWPI Center for Materials Nanoarchitectonics (WPI-MANA), National Institute for Materials Science (NIMS), Namiki 1-1, Tsukuba 305-0044, Japan.

^dScience Island Branch of Graduate School, University of Science and Technology of China, Hefei 230026, China.

^eInstitute for Computational Materials Science, School of Physics and Electronics, Henan University, Kaifeng 475004, China

*E-mail: jeff.snyder@northwestern.edu, yshzhang@theory.issp.ac.cn

Table S1: Cross validation score (CV, meV/mixing atom) and effective cluster interactions (ECI) (meV/atom) for $\text{TiFe}_{1-x}\text{Ni}_x\text{Sb}$, $\text{ZrFe}_{1-x}\text{Ni}_x\text{Bi}$ and $\text{VFe}_{1-x}\text{Ni}_x\text{Ge}$ systems. The triplets are identify according to their longest side, the other two sides being the first-nearest neighbors.

System	CV	1st pair	2nd pair	3rd pair	4th pair	1st triplet	2nd triplet
$\text{TiFe}_{1-x}\text{Ni}_x\text{Sb}$	29.227	0.043	0.016	0.002	0.005	0.000	0.000
$\text{ZrFe}_{1-x}\text{Ni}_x\text{Bi}$	25.816	0.035	0.022	0.005	0.007	-0.014	0.013
$\text{VFe}_{1-x}\text{Ni}_x\text{Ge}$	27.340	0.030	0.022	-0.005	0.000	0.0002	0.000

Table S2: DFT predicted SQS structures (space group: P1) of $\text{Ti}_{16}\text{Fe}_8\text{Ni}_8\text{Sb}_{16}$ ($a=7.260 \text{ \AA}$, $b=8.379 \text{ \AA}$, $c=13.874 \text{ \AA}$) and $\text{V}_{16}\text{Fe}_8\text{Ni}_8\text{Ge}_{16}$ ($a=6.79326 \text{ \AA}$, $b=7.843 \text{ \AA}$, $c=12.998 \text{ \AA}$).

System	Atom	x	y	z
$\text{Ti}_4\text{Fe}_2\text{Ni}_2\text{Sb}_4$	Ti	0.1875	0.0000	0.4375
	Ti	0.4375	0.0000	0.6875
	Ti	0.1875	0.2500	0.9375
	Ti	0.6875	0.0000	0.9375
	Ti	0.4375	0.2500	0.1875
	Ti	0.9375	0.0000	0.1875
	Ti	0.1875	0.5000	0.4375
	Ti	0.6875	0.2500	0.4375
	Ti	0.4375	0.5000	0.6875
	Ti	0.9375	0.2500	0.6875
	Ti	0.1875	0.7500	0.9375
	Ti	0.6875	0.5000	0.9375
	Ti	0.4375	0.7500	0.1875
	Ti	0.9375	0.5000	0.1875
	Ti	0.6875	0.7500	0.4375
	Ti	0.9375	0.7500	0.6875
	Fe	0.2500	0.0000	0.2500
	Fe	0.5000	0.0000	0.5000
	Fe	0.2500	0.2500	0.7500
	Fe	0.5000	0.2500	0.0000
	Fe	0.0000	0.7500	0.5000
	Fe	0.5000	0.5000	0.5000
	Fe	0.2500	0.7500	0.7500
	Fe	0.7500	0.5000	0.7500
	Ni	0.0000	0.0000	0.0000
	Ni	0.0000	0.5000	0.0000
	Ni	0.5000	0.7500	0.0000
	Ni	0.7500	0.2500	0.2500
	Ni	0.2500	0.5000	0.2500
	Ni	0.7500	0.7500	0.2500
	Ni	0.0000	0.2500	0.5000
	Ni	0.7500	0.0000	0.7500
	Sb	0.0625	0.0000	0.8125
	Sb	0.3125	0.0000	0.0625
	Sb	0.0625	0.2500	0.3125
	Sb	0.5625	0.0000	0.3125
	Sb	0.3125	0.2500	0.5625
	Sb	0.8125	0.0000	0.5625
	Sb	0.0625	0.5000	0.8125
	Sb	0.5625	0.2500	0.8125
Sb	0.3125	0.5000	0.0625	
Sb	0.8125	0.2500	0.0625	
Sb	0.0625	0.7500	0.3125	
Sb	0.5625	0.5000	0.3125	
Sb	0.3125	0.7500	0.5625	

	Sb	0.8125	0.5000	0.5625
	Sb	0.5625	0.7500	0.8125
	Sb	0.8125	0.7500	0.0625
$V_{16}Fe_8Ni_8Sb_{16}$	V	0.1875	0.0000	0.4375
	V	0.4375	0.0000	0.6875
	V	0.1875	0.2500	0.9375
	V	0.6875	0.0000	0.9375
	V	0.4375	0.2500	0.1875
	V	0.9375	0.0000	0.1875
	V	0.1875	0.5000	0.4375
	V	0.6875	0.2500	0.4375
	V	0.4375	0.5000	0.6875
	V	0.9375	0.2500	0.6875
	V	0.1875	0.7500	0.9375
	V	0.6875	0.5000	0.9375
	V	0.4375	0.7500	0.1875
	V	0.9375	0.5000	0.1875
	V	0.6875	0.7500	0.4375
	V	0.9375	0.7500	0.6875
	Fe	0.2500	0.0000	0.2500
	Fe	0.5000	0.0000	0.5000
	Fe	0.2500	0.2500	0.7500
	Fe	0.5000	0.2500	0.0000
	Fe	0.0000	0.7500	0.5000
	Fe	0.5000	0.5000	0.5000
	Fe	0.2500	0.7500	0.7500
	Fe	0.7500	0.5000	0.7500
	Ni	0.0000	0.0000	0.0000
	Ni	0.0000	0.5000	0.0000
	Ni	0.5000	0.7500	0.0000
	Ni	0.7500	0.2500	0.2500
	Ni	0.2500	0.5000	0.2500
	Ni	0.7500	0.7500	0.2500
	Ni	0.0000	0.2500	0.5000
	Ni	0.7500	0.0000	0.7500
	Ge	0.0625	0.0000	0.8125
	Ge	0.3125	0.0000	0.0625
	Ge	0.0625	0.2500	0.3125
	Ge	0.5625	0.0000	0.3125
	Ge	0.3125	0.2500	0.5625
	Ge	0.8125	0.0000	0.5625
	Ge	0.0625	0.5000	0.8125
	Ge	0.5625	0.2500	0.8125
	Ge	0.3125	0.5000	0.0625
	Ge	0.8125	0.2500	0.0625
	Ge	0.0625	0.7500	0.3125
	Ge	0.5625	0.5000	0.3125
	Ge	0.3125	0.7500	0.5625
	Ge	0.8125	0.5000	0.5625

Ge	0.5625	0.7500	0.8125
Ge	0.8125	0.7500	0.0625

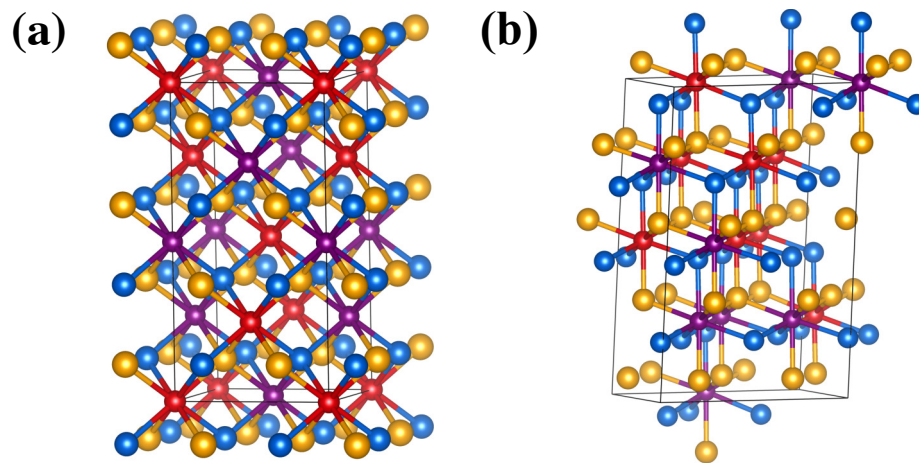


Fig. S1: Crystal structures of ordered $V_4Fe_2Ni_2Ge_4$ and SQS $V_{16}Fe_8Ni_8Ge_{16}$. The blue, red, purple and yellow spheres represent the V, Fe, Ni and Ge atoms, respectively.

Although the deformation potential (DP) theory might provide the better electronic relaxation time, it depends on the deformation potential, effective mass and velocity^a. The symmetry of the band extreme would define several deformation potentials. Thus, it is not that easy to obtain an accurate deformation potential. On the other hand, for a large system with low symmetry, like the SQS structure, its band structure is usually too complicated to define a good deformation potential. Additionally, it is time-consuming to calculate the phonon velocity of the SQS structures. We obviously need a convenient way, such as the constant relaxation time. To valid the constant relaxation time approximation, we use the DP theory to calculate the electronic relaxation times of a ground state structure. For a ground state structure $V_4Fe_2Ni_2Ge_4$, (Fig. S2), we notice that its electron relaxation time calculated using DP is around 10 fs , which is close to the constant relaxation time (10 fs). Therefore, it is reasonable and convenient to use the constant relaxation time approximation to evaluate the electrical properties.

^aBardeen, J.; Shockley, W. Deformation Potentials and Mobilities in Non-Polar Crystals. Phys. Rev. 1950, 80, 72.

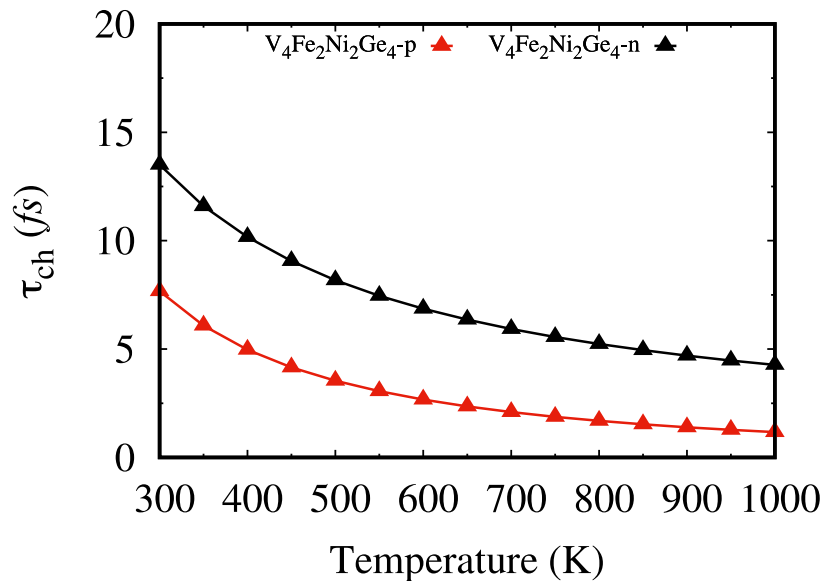


Fig. S2: Temperature dependent electronic relaxation times of ordered $Ti_4Fe_2Ni_2Sb_4$ and $V_4Fe_2Ni_2Ge_4$. The void and solid circles and triangles represent the results by constant relaxation approximation ($\tau_{ch}=10 fs$) and deformation potential method, respectively.

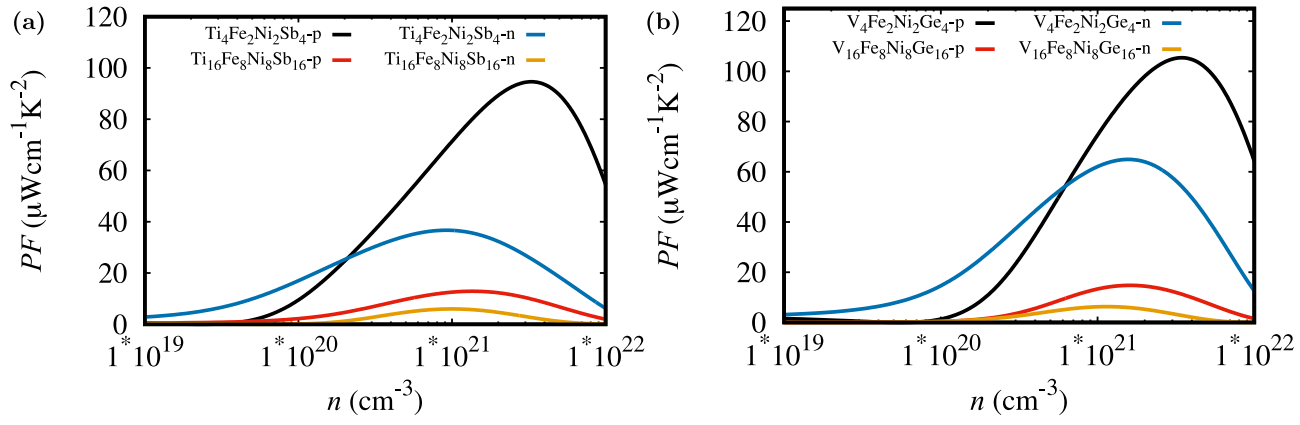


Fig. S3: Carrier concentration dependent power factors of ordered ground states ($\text{Ti}_4\text{Fe}_2\text{Ni}_2\text{Sb}_4$ and $\text{V}_4\text{Fe}_2\text{Ni}_2\text{Ge}_4$) and SQS structures ($\text{Ti}_{16}\text{Fe}_8\text{Ni}_8\text{Sb}_{16}$ and $\text{V}_{16}\text{Fe}_8\text{Ni}_8\text{Ge}_{16}$).

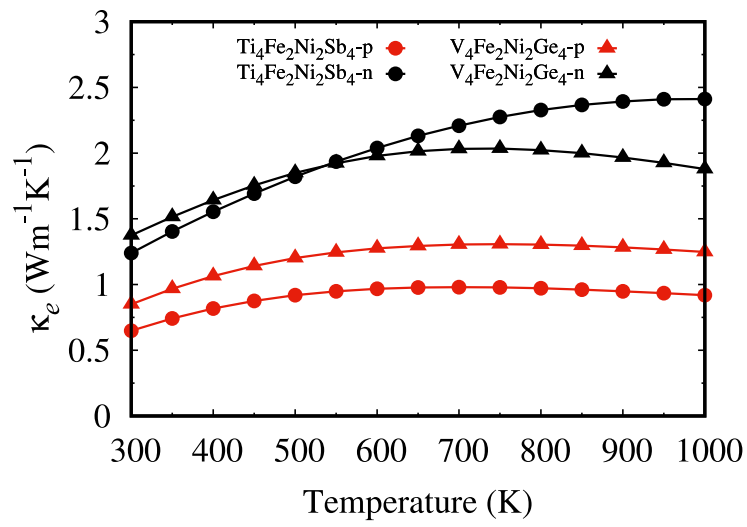


Fig. S4: Temperature dependent electronic thermal conductivities of ordered $\text{Ti}_4\text{Fe}_2\text{Ni}_2\text{Sb}_4$ (circles) and $\text{V}_4\text{Fe}_2\text{Ni}_2\text{Ge}_4$ (triangles).

Weighted mobility is a better descriptor of the inherent electrical transport properties, which is defined as^b

$$\mu_W = 331 \frac{\text{cm}^2}{\text{Vs}} \left(\frac{m\Omega\text{cm}}{\rho} \right) \left(\frac{T}{300\text{K}} \right) \left[\frac{\exp \left[\frac{|S|}{k_B/e} - 2 \right]}{1 + \exp \left[-5 \frac{|S|}{k_B/e} - 1 \right]} + \frac{\frac{3}{\pi^2} \frac{|S|}{k_B/e}}{1 + \exp \left[5 \frac{|S|}{k_B/e} - 1 \right]} \right] \quad (1)$$

where ρ is the electrical resistivity (unit: $m\Omega\text{ cm}$), S the Seebeck coefficient and $k_B/e = 86.3\ \mu\text{V K}^{-1}$. Temperature dependent weighted mobilities of $\text{Ti}_4\text{Fe}_2\text{Ni}_2\text{Sb}_4$ and $\text{V}_4\text{Fe}_2\text{Ni}_2\text{Ge}_4$ are given in Fig. S5.

^bG. J. Snyder, A. H. Snyder, M. Wood, R. Gurunathan, B. H. Snyder and C. Niu, Weighted Mobility, *Adv. Mater.*, 2020, 2001537.

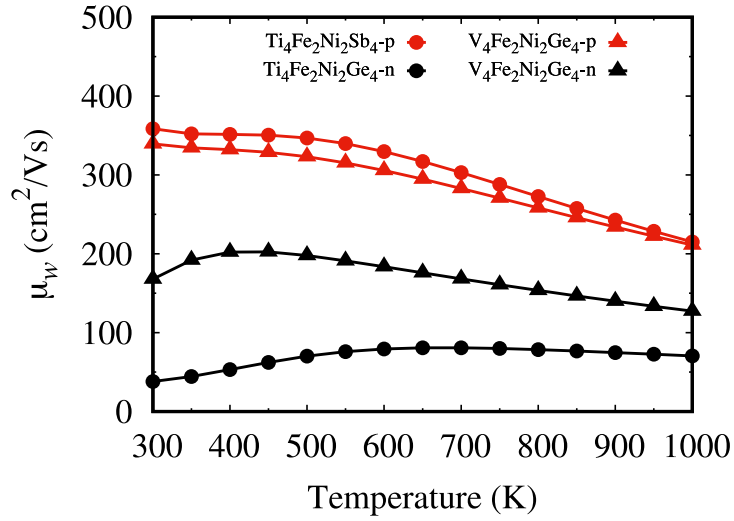


Fig. S5: Temperature dependent weighted mobilities of $\text{Ti}_4\text{Fe}_2\text{Ni}_2\text{Sb}_4$ (circles) and $\text{V}_4\text{Fe}_2\text{Ni}_2\text{Ge}_4$ (triangles).